 CMES, vol.7, no.1, pp.85-95, 2005

A New Fast Multipole Boundary Element Method for Large Scale Analysis of Mechanical Properties in 3D Particle-Reinforced Composites

Haitao Wang[1] **and Zhenhan Yao**[1]

Abstract: This paper addresses a new boundary element method (BEM) for the numerical analysis of mechanical properties in 3D particle-reinforced composites. The BEM is accelerated by a new version fast multipole method (FMM) in order to perform large scale simulation of a representative volume element (RVE) containing up to several hundred randomly distributed elastic spherical particles on only one personal computer. The maximum number of degrees of freedom (DOF) reaches more than 300,000. Efficiency of the developed new version fast multipole BEM code is evaluated compared with other conventional solutions for BEM. The effects of micro-structural parameters, namely the particle size, particle/matrix moduli ratio and particle volume fraction on the effective elastic moduli and interfacial stress fields are studied. The numerical results show that fast multipole BEM is a promising tool for large scale analysis of overall mechanical properties and micro-structural details in such kind of composites, when the particles and matrix are assumed to be elastic. Based on the present work, future investigations could be extended to simulation on brittle fracture process.

keyword: Boundary element method, particle-reinforced composites, interfacial stress, fast multipole method.

1 Introduction

Particle-reinforced composites are used increasingly in various industrial applications, leading to much interest and the corresponding research in the simulation of these materials. Numerous models are presented to study the effects of micro-structural parameters on the macro properties and possible fracture modes in particle-reinforced composites. In order to estimate the effective elastic properties of these composite materials, various theoretical methods have been developed by researchers [Budiansky (1965), Hill (1965), Mori and Tanaka (1973), Weng (1984), Huang, Hu, Wei, and Chandra (1994)] based on simplified models. At the same time, some numerical schemes have been presented for models with more general shapes [Isida and Igawa (1991), Day, Snyder, Garboczi, and Thorpe (1992), Yuji, Hirotada, and Tetsuharu (2000)] and the corresponding numerical results are in general agreement with that of theoretical ones in some special cases.

However, the modeling and evaluation of particle-reinforced composites still meet some difficulties. There are many micro-structural factors in real composite materials that may be crucial to macro behaviors, such as particle account, particle size, volume fraction, moduli ratio of particle/matrix, etc. In order to have a deep understanding of the effects of these factors on effective mechanical properties and stress distributions in a real composite, large scale models with detailed micro-structures that are controlled by these factors are preferred in many situations. Unfortunately, a 3D representative volume element (RVE) with up to several hundred randomly distributed particles is too complicated for theoretical models and beyond the ability of many current numerical schemes. Most numerical analysis reported in literatures is based on a 2D model with several circles or a 3D model with only a few particles. Therefore, large scale simulation of 3D many particle-reinforced composites with an acceptable amount of computer resources is challenging, motivating our research in this paper.

Among various numerical schemes, BEM is particularly suitable for the simulation of particle-reinforced composites because of dimension reduction and high accuracy [Kong, Yao, and Zheng (2002)]. Using BEM, only the outer surface of the matrix and the particle/matrix interfaces need to be discretized. Therefore, the corresponding problem size is greatly reduced compared with other volume discretization based schemes, such as finite element method (FEM). With the development of fast multi-

[1] Dept. Engineering Mechanics, Tsinghua Univ., Beijing, China

pole method (FMM) as a fast solver for BEM, large scale simulation with more than 100,000 unknowns could be achieved readily on only one desktop computer. Rokhlin and Greengard presented FMM [Rokhlin (1985), Greengard and Rokhlin (1997a)] for potential problems and have done extensive research for various application of FMM. Several $O(NlogN)$ and $O(N)$ algorithms based on FMM were reported for the simulation of elastic problems [Yamada and Hayami (1995), Peirce and Napier (1995), Fu, Klimkowski, Rodin, Berger, Browne, Singer, Geijn, and Vernaganti (1998), Popov and Power (2001)], crack problems [Nishimura, Yoshida, and Kobayashi (1999), Yoshida, Nishimura, and Kobayashi (2001a), Lai and Rodin (2003)] and some extended features, such as the Symmetric Galerkin BEM [Aimi, Diligenti, Lunardini, and Salvadori (2003)] and the BEM with nonlinear boundary conditions [Aoki, Amaya, Urago, and Nakayama (2004)]. In order to further improve the efficiency of FMM, Rokhlin (1990) introduced the concept of diagonal forms for 2D FMM. Epton and Dembart (1995) gave a more detailed mathematical description of these diagonal forms. In the late 1990s, a new version FMM is developed, achieving satisfactory improvement of FMM in both 2D and 3D models. The corresponding researches are found in Hrycak and Rokhlin (1998) for 2D Laplace equation, Greengard and Rokhlin (1997b) and Cheng, Greengard, and Rokhlin (1999) for 3D Laplace equation. Nishimura, Miyakoshi, and Kobayashi (1999) applied the new version FMM accelerated BEM to crack problems for the 2D Laplace equation, and Yoshida, Nishimura, and Kobayashi (2001b) for the 3D Laplace equation. Among numerous applications of fast multipole BEM, some attempts have been made for the large scale analysis of particle- and fiber-reinforced composites. In authors' group, fast multipole BEM was applied to the simulation of 2D solids with randomly distributed circular inclusions [Wang and Yao (2004)]. Models in numerical examples contain up to 1,600 elastic inclusions. Liu, Nishimura, Otani, Takahashi, Chen, and Munakata (2004) used FMM accelerated BEM for the simulation of rigid fibers in a 3D infinite elastic medium. Models in their paper contain above 5,800 rigid inclusions.

In the present paper, the large scale simulation of effective mechanical properties and stress distributions in 3D particle-reinforced composites is performed using BEM accelerated by a new version fast multipole method. The numerical schemes presented include a similar sub-domain BEM approach [Kong, Yao, and Zheng (2002)], which is suitable for modeling elastic particles, and a new version fast multipole BEM for 3D elasticity to simulate the finite elastic domain with several hundred elastic particles on only one personal computer. A representative model in the numerical examples is an elastic cubic matrix containing a large number of randomly distributed elastic spherical particles. The maximum number of unknowns reaches above 300,000. In the numerical tests, the effects of various micro-structural parameters, such as particle size, volume fraction, particle/matrix moduli ratio, etc on the effective elastic moduli and stress distributions of the composites are evaluated. The numerical results show that fast multipole BEM is a powerful tool for large scale simulation and deeper understanding of details in particle-reinforced composites. This method may help carry out further research in the field of such composite materials.

2 Repeated similar sub-domain BEM for elastic solids containing elastic particles

The model of a 3D elastic matrix containing n randomly distributed elastic spherical particles of the same size is shown in Fig. 1. Let V_0 denote the sub-domain of the matrix, $V_1, V_2, \ldots, V_n$ the sub-domains of particles, S_0 the outer boundary of the matrix, and S_k the particle/matrix interface of the k-th particle. In addition, Let S_0^U and S_0^T denote outer boundary parts of the matrix with given displacement and given traction, respectively. The boundary integral equations for 3D elasticity without body force are expressed for the matrix and the k-th particle, respectively,

$$C_{ij}(x)u_j(x) + \int_{S_0+\sum S_k} T_{ij}^0(x,y)u_j(y)\,dS(y) = \int_{S_0+\sum S_k} U_{ij}^0(x,y)t_j(y)\,dS(y) \tag{1}$$

$$C_{ij}(x)u_j(x) + \int_{S_k} T_{ij}^k(x,y)u_j(y)\,dS(y) = \int_{S_k} U_{ij}^k(x,y)t_j(y)\,dS(y) \tag{2}$$

where x and y denote the source point and field point on the boundary, respectively. Superscripts 0 and k indicate the matrix and the k-th particle sub-domain, respectively. Subscripts $i, j = 1, 2, 3$. $C_{ij}(x)$ is a free term

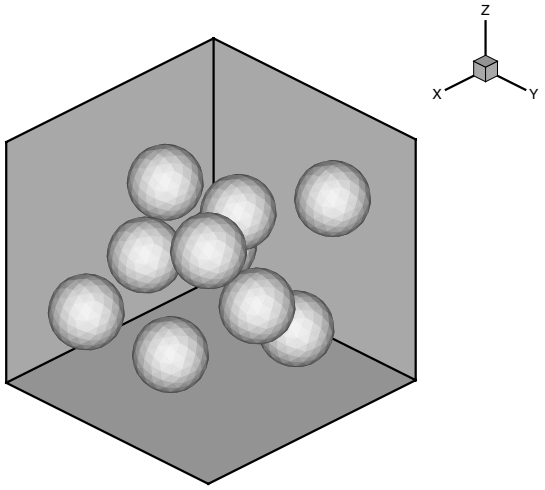

Figure 1 : A 3D model with spherical particles

related to the shape of the boundary at point x. If the boundary is smooth at point x, $C_{ij}(x) = \delta_{ij}/2$. u_i and t_i denote the boundary displacement and traction, respectively. $U_{ij}(x,y)$ and $T_{ij}(x,y)$ are fundamental solutions for 3D elasticity expressed as,

$$U_{ij}(x,y) = \frac{1}{16\pi G(1-v)r}\left[(3-4v)\,\delta_{ij} + r_{,i}\,r_{,j}\right],$$
$$T_{ij}(x,y) = \frac{1}{8\pi(1-v)r^2}\Big\{(1-2v)\,(r_{,j}\,n_i - r_{,i}\,n_j)$$
$$-\frac{\partial r}{\partial n}\left[(1-2v)\delta_{ij} + 3r_{,i}\,r_{,j}\right]\Big\} \tag{3}$$

where r is the distance between source point x and field point y, $r = \sqrt{r_i r_i}$, $r_i = y_i - x_i$. G is shear modulus and v is Poisson's ratio. After discretization with piecewise constant, linear or quadratic boundary elements, Eqs. 1 and 2 can be written into matrix forms as follows,

$$\left[A_1^0\,A_2^0\,A_3^1\,\cdots\,A_3^k\,\cdots\,A_3^n\right]\left[U_0\,T_0\,U_1\,\cdots\,U_k\,\cdots\,U_n\right]^T$$
$$= \left[B_1^0\,B_2^0\,B_3^1\,\cdots\,B_3^k\,\cdots\,B_3^n\right]\left[\overline{T}_0\,\overline{U}_0\,T_{10}\,\cdots\,T_{k0}\,\cdots\,T_{n0}\right]^T \tag{4}$$

$$H^k U_k = G^k T_{kk} \tag{5}$$

where U_0 and $\overline{T}_0$ stand for the unknown nodal displacement and given nodal traction on S_0^T, respectively, T_0 and $\overline{U}_0$ the unknown nodal traction and given nodal displacement on S_0^U, respectively, U_k the unknown nodal displacement on S_k. T_{k0} and T_{kk} stand for the unknown nodal traction on S_k for the matrix and the k-th particle, respectively. Sub matrices A, B in Eq. 4 consist of entries for the matrix material sub-domain, H^k, G^k in Eq. 5 for the k-th particle material sub-domain. Considering the interface condition for traction, one can obtain,

$$T_{k0} = -T_{kk} = -\left[\left(G^k\right)^{-1} H^k\right] U_k = -D^k U_k \tag{6}$$

where D^k is an incidence matrix expressing the relations between T_{k0} and U_k. Substituting Eq. 6 into Eq. 4, one can obtain the final equation system for 3D elastic solids with elastic particles as follows,

$$\left[A_1^0\,A_2^0\,\overline{A_3^1}\,\cdots\,\overline{A_3^k}\,\cdots\,\overline{A_3^n}\right]\left[U_0\,T_0\,U_1\,\cdots\,U_k\,\cdots\,U_n\right]^T$$
$$= \left[B_1^0\,B_2^0\right]\left\{\begin{array}{c}\overline{T}_0\\ \overline{U}_0\end{array}\right\} \tag{7}$$

where

$$\overline{A_3^k} = A_3^k + B_3^k D^k, \quad k = 1,\ldots,n \tag{8}$$

If all the randomly distributed particles are of the same size and material, the corresponding incidence matrices D^k are also identical. Therefore, D^k is required to be formed only once for one particle, and reused directly for all other particles. If all the particles have different sizes and materials, D^k can also be calculated only once because of the similar relationship between particle phases of different sizes and materials, which can be expressed as follows, with the assumption that Poisson's ratio is the same,

$$D^{k+1} = \frac{E^{k+1}}{E^k}\cdot\frac{r^k}{r^{k+1}}\cdot D^k \tag{9}$$

where E^k and r^k are Young's modulus and radius of the k-th particle, respectively.

3 Fast multipole BEM for 3D elasticity

In this section, we give a brief introduction to the basic concepts of fast multipole BEM for 3D elasticity.

Conventional BEM is not efficient for problems of large size because the coefficient matrix arising from BEM is dense and sometimes asymmetric. Solving such equation system requires $O(N^2)$ memory and $O(N^3)$ operations using direct solvers such as Gauss elimination, where N is the number of unknowns. As N increases, the memory and computation time increase rapidly. Therefore, direct solvers scale poorly with increasing problem sizes. Fortunately, fast multipole method makes it possible for BEM to perform large scale simulations with $O(N)$ resources. The crucial structure in 3D fast multipole BEM is an adaptive octal-tree. During the procedures of iterative solutions for BEM, such as GMRES, information of the coefficient matrix-vector multiplication in each iterative step is obtained by recursive operations on this tree structure. Therefore, the coefficient matrix is not explicitly available using fast multipole BEM. Operations and memory requirement of this tree only cost $O(N)$, thus total costs of the iterative solution are reduced to $O(N)$.

Three basic concepts of FMM, namely the multipole expansion, local expansion and exponential expansion, are brief discussed for the case of 3D elasticity as follows.

3.1 Multipole expansion

The two boundary integrals $\int_S U_{ij}(x,y)t_j(y)\,dS(y)$ and $\int_S T_{ij}(x,y)u_j(y)\,dS(y)$ in Eqs. 1 and 2 stand for the contribution of field point y to source point x. Locate y in a cube $\mathbf{A}$, whose center is y_0, as shown in Fig. 2. Assume the following threshold is satisfied,

$$|\overrightarrow{y_0y}| \le \frac{1}{2}|\overrightarrow{y_0x}|, \quad \forall y \in \mathbf{A} \tag{10}$$

The fundamental solution $U_{ij}(x,y)$ is expanded with respect to y around y_0, as shown in the following generalized form,

$$U_{ij}(x,y) = \sum_n \sum_m f_{nm}(x,y_0)g_{nm}(y,y_0) \tag{11}$$

where the former part $f_{nm}(x,y_0)$ is only related to x and the latter part $g_{nm}(y,y_0)$ is only related to y.

As one example, a detailed expression of Eq. 11 is given in literature [Yoshida (2001)] as,

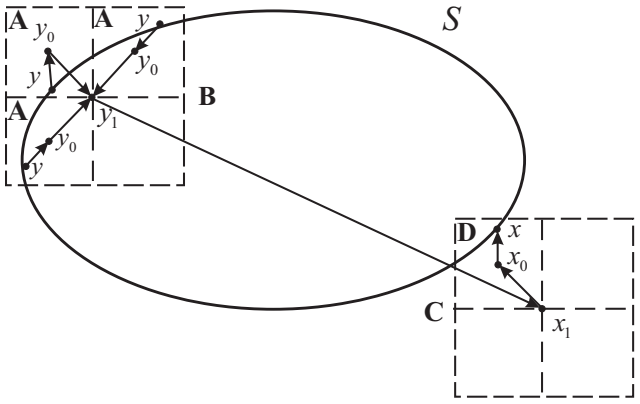

Figure 2 : Basic procedures of FMM

$$U_{ij}(x,y) = \frac{1}{8\pi G}\sum_{n=0}^{\infty}\sum_{m=-n}^{n}\left[\overline{F^S_{ij,nm}}(\overrightarrow{y_0x})\,R_{nm}(\overrightarrow{y_0y}) + \overline{G^S_{i,nm}}(\overrightarrow{y_0x})\,(\overrightarrow{y_0y})_j\,R_{nm}(\overrightarrow{y_0y})\right] \tag{12}$$

where

$$F^S_{ij,nm}(\overrightarrow{y_0x}) = \frac{\lambda+3G}{\lambda+2G}\delta_{ij}S_{nm}(\overrightarrow{y_0x}) - \frac{\lambda+G}{\lambda+2G}(\overrightarrow{y_0x})\frac{\partial}{\partial x_i}S_{nm}(\overrightarrow{y_0x})$$
$$G^S_{i,nm}(\overrightarrow{y_0x}) = \frac{\lambda+G}{\lambda+2G}\frac{\partial}{\partial x_i}S_{nm}(\overrightarrow{y_0x}) \tag{13}$$

R_{nm} and S_{nm} are solid harmonic functions defined in literature [Yoshida (2001)], and $\overline{(\,)}$ stands for the complex conjugate.

Substituting Eq. 11 into the boundary integral $\int_S U_{ij}(x,y)t_j(y)\,dS(y)$, one can obtain,

$$\int_S U_{ij}(x,y)t_j(y)\,dS(y) = \int_S\left[\sum_n\sum_m f_{nm}(x,y_0)g_{nm}(y,y_0)\right]t_j(y)\,dS(y) = \sum_n\sum_m f_{nm}(x,y_0)c_{nm}(y_0) \tag{14}$$

where

$$c_{nm}(y_0) = \int_S g_{nm}(y,y_0)t_j(y)\,dS(y) \tag{15}$$

$c_{nm}(y_0)$ series are called multipole moments, which are formed only once and reused to obtain the integral for different source point x using Eq. 14.

Another boundary integral $\int_S T_{ij}(x,y)u_j(y)\,dS(y)$ has a similar form of expansion to Eq. 14.

Let **B** denote a parent cube of **A**, as shown in Fig. 2. y_1 is **B**'s center. Assume the following threshold is satisfied,

$$|\overrightarrow{y_1y}| \le \frac{1}{2}|\overrightarrow{y_1x}|, \quad \forall y \in \mathbf{B} \tag{16}$$

Using expansion of $U_{ij}(x,y)$ with respect to y around y_1, one can obtain a similar expansion to Eq. 14 as,

$$\int_S U_{ij}(x,y)t_j(y)\,dS(y) = \sum_n \sum_m f_{nm}(x,y_1)c_{nm}(y_1) \tag{17}$$

where the new multipole moments $c_{nm}(y_1)$ can be calculated directly by the old multipole moments $c_{nm}(y_0)$.

3.2 Local expansion

Let **C** denote a cube of the same size as **B**, as shown in Fig. 2. x_1 is **C**'s center. Assume the following threshold is satisfied,

$$|\overrightarrow{x_1x}| \le \frac{1}{2}|\overrightarrow{x_1y_1}|, \quad \forall x \in \mathbf{C} \tag{18}$$

$f_{nm}(x,y_1)$ in Eq. 17 is expanded with respect to x around x_1, as shown in the following generalized form,

$$f_{nm}(x,y_1) = \sum_{n'} \sum_{m'} p_{n'm'}(x,x_1)q^{nm}_{n'm'}(y_1,x_1) \tag{19}$$

where the former part $p_{n'm'}(x,x_1)$ is only related to x and the latter part $q^{nm}_{n'm'}(y_1,x_1)$ is only related to y_1. Substituting Eq. 19 into Eq. 17, one can obtain a new expansion as,

$$\begin{aligned}
&\int_S U_{ij}(x,y)t_j(y)\,dS(y) \\
&= \sum_n \sum_m \left[\sum_{n'} \sum_{m'} p_{n'm'}(x,x_1)q^{nm}_{n'm'}(y_1,x_1) \right] c_{nm}(y_1) \\
&= \sum_{n'} \sum_{m'} p_{n'm'}(x,x_1)d_{n'm'}(x_1)
\end{aligned} \tag{20}$$

where

$$d_{n'm'}(x_1) = \sum_n \sum_m q^{nm}_{n'm'}(y_1,x_1)c_{nm}(y_1) \tag{21}$$

$d_{n'm'}(x_1)$ series are called local moments, which are calculated directly by multipole moments $c_{nm}(y_1)$. Local moments are formed only once and reused for different source point x using Eq. 20.

Let **D** denote a child cube of **C**, as shown in Fig. 2. x_0 is **D**'s center. Using expansion of $f_{nm}(x,y_1)$ with respect to x around x_0, one can obtain a similar expansion to Eq. 20 as,

$$\int_S U_{ij}(x,y)t_j(y)\,dS(y) = \sum_{n'} \sum_{m'} p_{n'm'}(x,x_0)d_{n'm'}(x_0) \tag{22}$$

where the new local moments $d_{n'm'}(x_0)$ can be calculated directly by the old local moments $d_{n'm'}(x_1)$.

3.3 Exponential expansion

The concept of exponential expansion is only available for a new version FMM developed in the late 1990s [Hrycak and Rokhlin (1998), Greengard and Rokhlin (1997b),Cheng, Greengard, and Rokhlin (1999)]. In procedures of the new version, the dense translation operator from multipole moments to local moments in Eq. 21 are diagonalized by three new steps, which are described as: 1). multipole to exponential shift in order to obtain a new series of exponential moments by multipole moments in the same cube, 2). exponential to exponential shift in order to transfer exponential moments from one cube containing field points to another cube containing source points, 3). exponential to local shift in order to obtain local moments by exponential moments in the same cube. Fig. 3 shows these three steps. Since operations needed in FMM to obtain local moments by multipole moments dominate most computer resources for 3D problems, successful simplification of these operations makes the new version FMM much effective than the original one.

3.4 Tree structure

An adaptive octal-tree is used in FMM for 3D problems in order to store and retrieve multipole moments, local moments and exponential moments. The root of this tree stands for the biggest cube containing the whole model.

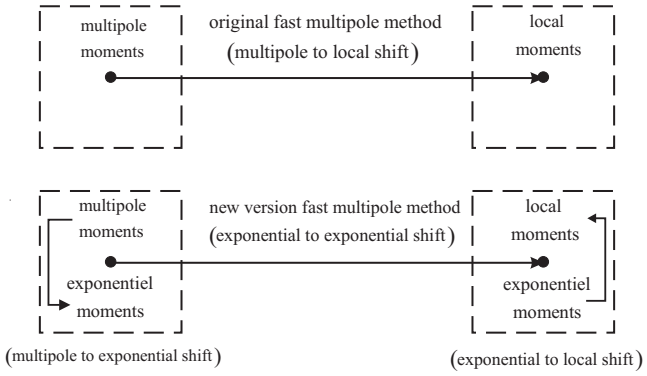

Figure 3 : Procedures of new version FMM

In order to form this tree automatically, the root is divided into eight identical sub-cubes. Each sub-cube is then divided recursively into smaller cubes until the number of boundary elements contained in a cube is less than a prescribed value. A cluster of this tree stands for a cube, and a leaf stands for a cube that needn't to be divided. Fig. 4 shows details of a model in an adaptive tree structure.

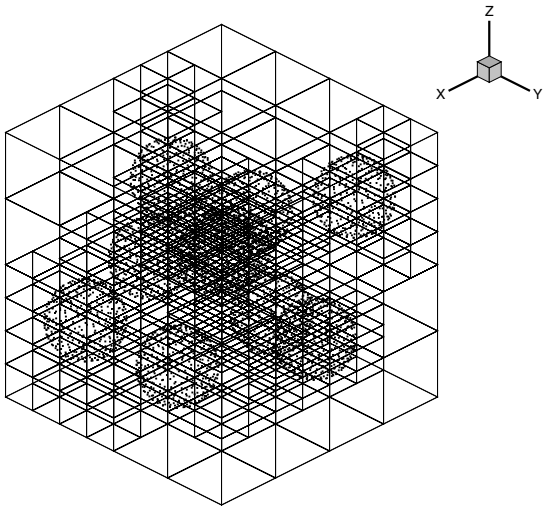

Figure 4 : Particles with an adaptive tree structure

Each cluster of this tree stores the corresponding multipole, local and exponential moments. In one iterative step of numerical solutions, an upward stage of the tree is applied to calculate multipole moments and a downward stage to calculate local and exponential moments. After preparation of all moments, the coefficient matrix-vector multiplication is obtained by recursive operations on this tree with $O(N)$ computational resources.

4 Numerical examples

The results of numerical examples are presented below. The code is written in ANSI C++ programming language and the corresponding program runs on a personal computer with one processor of Intel Pentium IV 3.0 GHz and 1GB memory.

4.1 Performance of a new version fast multipole BEM for 3D elasticity

The performance of parameters (CPU time and memory) on the number of DOFs using a new version fast multipole BEM for 3D elasticity is shown in Fig. 5. The corresponding results are also compared with a direct Gauss elimination solver based on LAPACK. A triangular piecewise constant boundary element type is used. The number of terms equals 10 for multipole and local expansion and 9 for exponential expansion. GMRES method is terminated when the residue is less than 1e-5, and the initial guess is a zero vector.

It can be seen from Fig. 5 that, CPU time and memory requirement using fast multipole BEM are approximately proportional to the number of DOFs. These observations demonstrate that both operations and storage of fast multipole BEM cost $O(N)$. In addition, the speed of fast multipole BEM is much faster than that of Gauss elimination when the problem size increases, while the corresponding memory requirement of fast multipole BEM is much smaller. Therefore, fast multipole BEM shows promising abilities to deal with large scale problems.

4.2 Interfacial stress distributions of 3D many particle-reinforced composites

Two representative volume elements containing different numbers of particles are investigated. Fig. 6 shows a model of one discretized particle with 350 triangular piecewise constant elements. Fig. 7 shows two cubic models with 100 and 300 randomly distributed particles, respectively. The maximum number of DOFs reaches 372,600. The side length of each cube is 20 mm and the particle volume fraction equals 10%. Normal tractions of $\sigma_{xx} = 1.0MPa$ are applied on the opposite sides of the cubes along X axis.

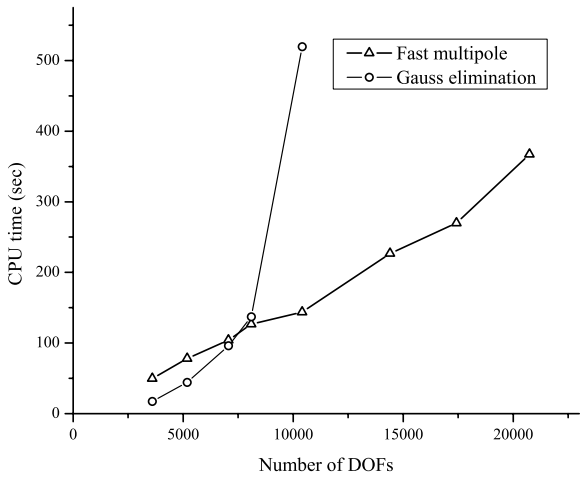

(a)

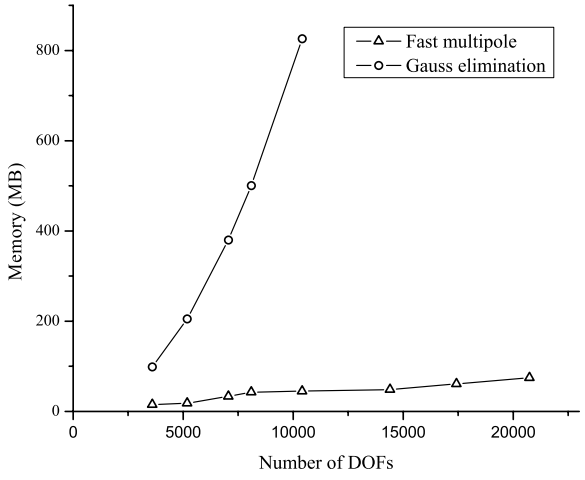

(b)

Figure 5 : (a) CPU time and (b) memory versus the number of DOFs

After carrying out the analysis, one can obtain the interfacial displacements readily and the corresponding interfacial stress distributions using Eq. 6. Fig. 8 and Fig. 9 show particle/matrix interfacial normal stress distributions and shear stress distributions of the two models, respectively, for the case of particle/matrix Young's moduli ratio $E_p/E_m = 5.0$. Note that high normal stresses are concentrated at tops of two opposite sides along X axis of each particle, while high shear stresses are concentrated at most areas of two opposites sides along X axis of each

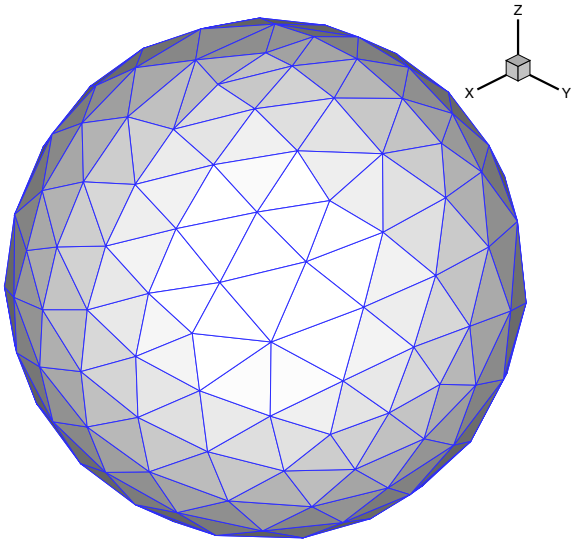

Figure 6 : A model of one discretized particle

particle except for two little polar areas where the shear stresses are relatively low.

4.3 Effective elastic modulus of 3D many particle-reinforced composites

The computational results for the effective Young's modulus and volume modulus of 3D solids with a large number of randomly distributed particles are presented and compared with some theoretical methods listed in literature [Kong, Yao, and Zheng (2002)], namely, the Mori-Tanaka method (M-T) and the interaction derivation method (IDD) . Fig. 10 and Fig. 11 shows the numerical solutions of different particle/matrix moduli ratios compared with some theoretical method for the case of a fixed volume fraction $c = 10\%$. Fig. 12 and Fig. 13 show the numerical solutions of different volume fractions and compared with some theoretical methods for the case of a fixed particle/matrix moduli ratio $E_p/E_m = 5.0$. The results show that numerical solutions using fast multipole BEM are in good agreement with M-T and IDD methods. For the effective volume modulus of the composites with stiffer spherical particles, the solution of M-T and IDD methods coincides with the H-S lower bound solution. But the numerical solutions of fast multipole BEM is slightly lower than the two analytical solutions and the H-S lower bound. This difference comes from the numerical errors of BEM, i.e., discretization error.

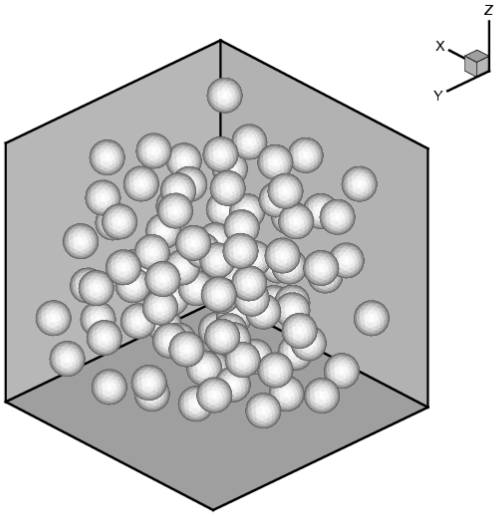

(a) 3D cube with 100 particles

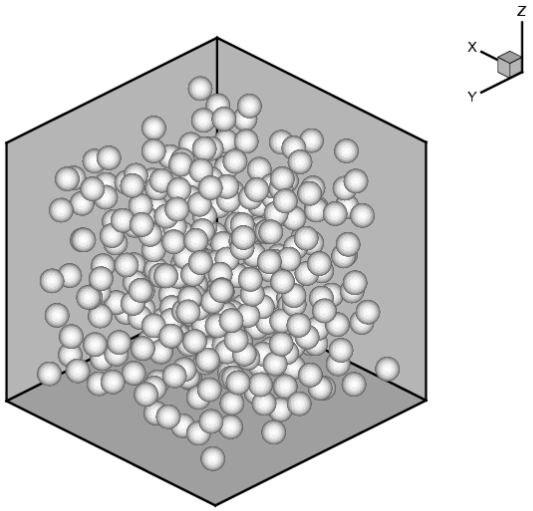

(b) 3D cube with 300 particles

Figure 7 : Two models with (a) 100 and (b) 300 particles

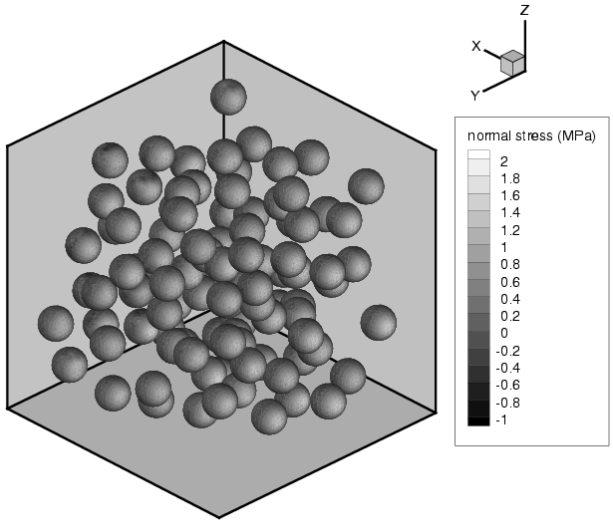

(a) 3D cube with 100 particles

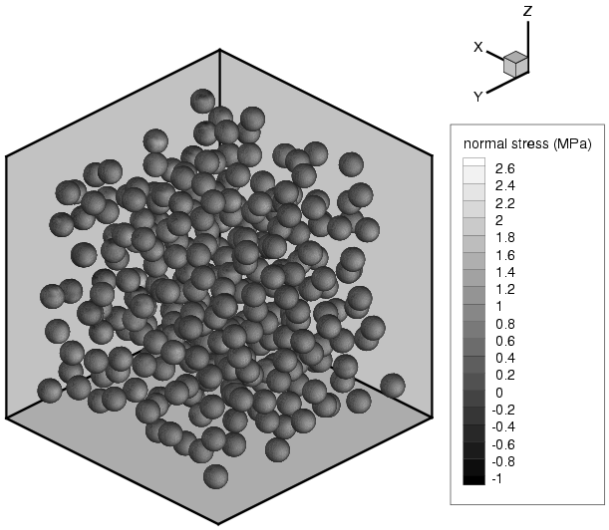

(b) 3D cube with 300 particles

Figure 8 : Interfacial normal stress distributions of (a) 100 particles and (b) 300 particles

Numerical examples show that as the boundary element mesh is further refined, the effective volume modulus obtained numerically increases to approach the H-S lower bound. This means that the numerical solution obtained by fast multipole BEM does not violate the theoretical lower bound.

4.4 Concluding Remarks

Repeated similar sub-domain BEM is used to simulate 3D particle-reinforced composites. By applying a new version fast multipole method to this field, 3D elastic solids containing up to several hundred randomly distributed elastic particles are analyzed on only one personal computer. The numerical tests clearly demonstrate efficiency of fast multipole BEM for large scale solutions

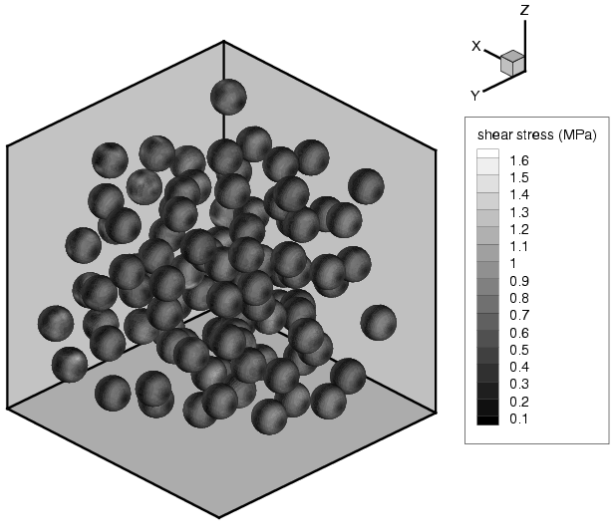

(a) 3D cube with 100 particles

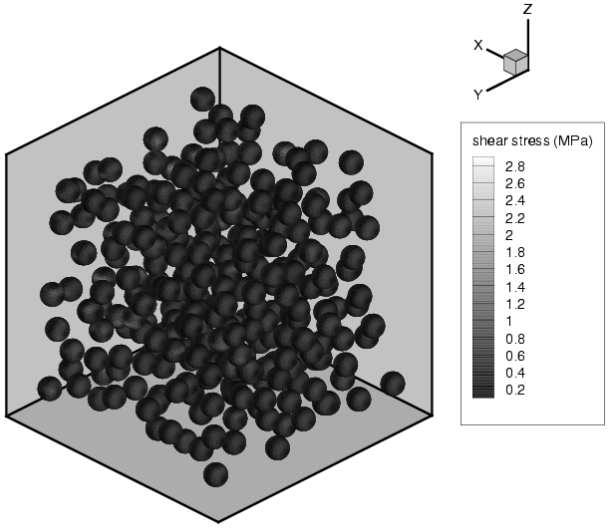

(b) 3D cube with 300 particles

Figure 9 : Interfacial shear stress distributions of (a) 100 particles and (b) 300 particles

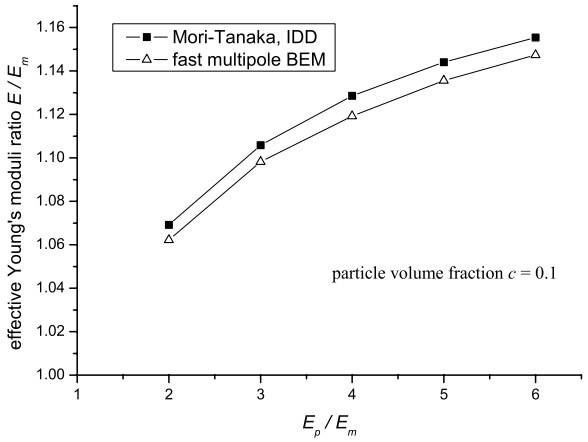

Figure 10 : Solutions of effective Young's modulus versus particle/matrix moduli ratio

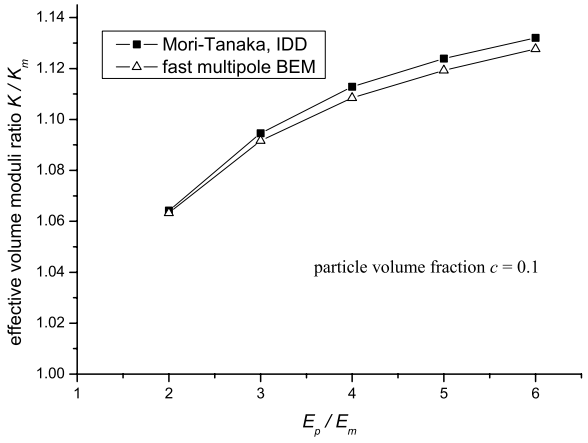

Figure 11 : Solutions of effective volume modulus versus particle/matrix moduli ratio

of such composites. Using this method, detailed interfacial stress distributions within the composites are readily obtained. In addition, the numerical results of effective Young's modulus and volume modulus are in good agreement with some theoretical methods.

Based on the present work on particle-reinforced composites, the developed multi-domain FMM BEM can be extended readily to the modeling and analysis of other composite materials, such as the large scale simulation of 3D composites with randomly distributed and oriented elastic fibers. Possible failure processes of such composite materials will also be concerned.

Acknowledgement: Financial support for the project from the National Natural Science Foundation of China, under grant No. 10172053 and the project from the Ministry of Education is gratefully acknowledged.

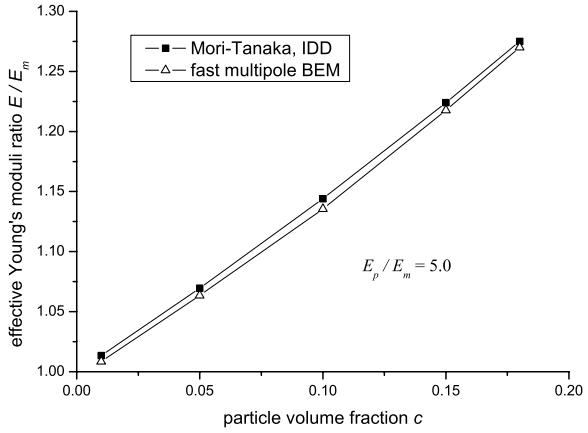

Figure 12 : Solutions of effective Young's modulus versus volume fraction

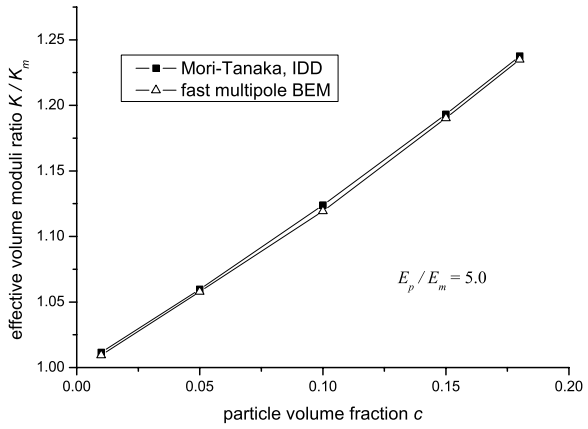

Figure 13 : Solutions of effective volume modulus versus volume fraction

References

Aimi, A.; Diligenti, M.; Lunardini, F.; Salvadori, A. (2003): A new application of the panel clustering method for 3D SGBEM. *CMES:Computer Modeling in Engineering & Sciences*, vol. 4, pp. 31–55.

Aoki, S.; Amaya, K.; Urago, M.; Nakayama, A. (2004): Fast multipole boundary element analysis of corrosion problems. *CMES:Computer Modeling in Engineering & Sciences*, vol. 6, no. 2, pp. 123–132.

Budiansky, Y. (1965): On the elastic moduli of heterogeneous materials. *J Mech Phys Solids*, vol. 13, pp. 223–227.

Cheng, H.; Greengard, L.; Rokhlin, V. (1999): A fast adaptive multipole algorithm in three dimensions. *J. Comput. Phys.*, vol. 155, pp. 468–498.

Day, A. R.; Snyder, K. A.; Garboczi, E. J.; Thorpe, M. F. (1992): The elastic moduli of a sheet containing circular holes. *J Mech Phys Solids*, vol. 40, pp. 1031–1051.

Epton, M. A.; Dembart, B. (1995): Multipole translation theory for the three-dimensional Laplace and Helmholtz equations. *SIAM J Sci Comput*, vol. 16, pp. 865–897.

Fu, Y. H.; Klimkowski, K. J.; Rodin, G. J.; Berger, E.; Browne, J. C.; Singer, J. K.; Geijn, R. A.; Vernaganti, K. S. (1998): A fast solution method for three-dimensional many-particle problems of linear elasticity. *Int J Numer. Methods Engng*, vol. 42, pp. 1215–1229.

Greengard, L.; Rokhlin, V. (1997): A fast algorithm for particle simulations. *J. Comput. Phys*, vol. 135, pp. 280–292.

Greengard, L.; Rokhlin, V. (1997): A new version of the fast multipole method for the Laplace equation in three dimensions. *Acta Numer*, vol. 6, pp. 229–270.

Hill, R. (1965): A self-consistent mechanics of composite materials. *J Mech Phys Solids*, vol. 13, pp. 213–222.

Hrycak, T.; Rokhlin, V. (1998): An improved fast multipole algorithm for potential fields. *SIAM J. Sci. Comput.*, vol. 19, pp. 1804–1826.

Huang, Y.; Hu, K. X.; Wei, X.; Chandra, A. (1994): A generalized self-consistent mechanics method for composite materials with multiphase inclusions. *J Mech Phys Solids*, vol. 42, pp. 491–504.

Isida, M.; Igawa, H. (1991): Analysis of zigzag array of circular holes in an infinite solid under uniaxial tension. *Int J Solids Struct*, vol. 27, pp. 849–864.

Kong, F. Z.; Yao, Z. H.; Zheng, X. P. (2002): BEM for simulation of a 2D elastic body with randomly distributed circular inclusions. *Acta Mech Solida Sinica*, vol. 15, no. 1, pp. 81–88.

Lai, Y. S.; Rodin, G. J. (2003): Fast boundary element method for three-dimensional solids containing many cracks. *Engrg. Anal. Boundary Elements*, vol. 27, pp. 845–852.

Liu, Y. J.; Nishimura, N.; Otani, Y.; Takahashi, T.; Chen, X. L.; Munakata, H. (2004): A fast boundary element method for the analysis of fiber-reinforced composites based on a rigid-inclusion model. *ASME Journal of Applied Mechanics*. (in press).

Mori, T.; Tanaka, K. (1973): Average stress in matrix and average elastic energy of materials with misfitting inclusions. *Acta Metall*, vol. 21, pp. 571–583.

Nishimura, N.; Miyakoshi, M.; Kobayashi, S. (1999): Application of new multipole boundary integral equation method to crack problems. In *Proc BTEC-99*, pp. 75–78. (in Japanese).

Nishimura, N.; Yoshida, K.; Kobayashi, S. (1999): A fast multipole boundary integral equation method for crack problems in 3D. *Engrg. Anal. Boundary Elements*, vol. 23, pp. 97–105.

Peirce, A. P.; Napier, J. A. L. (1995): A spectral multipole method for efficient solutions of large scale boundary element models in elastostatics. *Int. J. Numer. Methods Engng*, vol. 38, pp. 4009–4034.

Popov, V.; Power, H. (2001): An O(N) Taylor series multipole boundary element method for three-dimensional elasticity problems. *Engineering Analysis with Boundary Elements*, vol. 25, pp. 7–18.

Rokhlin, V. (1985): Rapid solution of integral equations of classical potential theory. *J Comput Phys*, vol. 60, pp. 187–207.

Rokhlin, V. (1990): Rapid solution of integral equations of scattering theory in two dimensions. *J Comput Phys*, vol. 86, pp. 414–439.

Wang, H. T.; Yao, Z. H. (2004): Application of a new fast multipole BEM for simulation of 2D elastic solid with large number of inclusions. *Acta Mechanica Sinica*, vol. 20, no. 6, pp. 613–622.

Weng, G. J. (1984): Some elastic properties of reinforced solids, with special reference to isotropic ones containing spherical inclusions. *Int J Engng Sci*, vol. 22, pp. 845–856.

Yamada, Y.; Hayami, K. (1995): A multipole boundary element Method for Two Dimensional Elastostatics. Technical Report METR 95-07, The University of Tokyo, Department of Mathematical Engineering and Information Physics, Faculty of Engineering, 1995.

Yoshida, K. (2001): *Applications of Fast Multipole Method to Boundary Integral Equation Method*. PhD thesis, Department of Global Environment Engineering, Kyoto University, 2001.

Yoshida, K.; Nishimura, N.; Kobayashi, S. (2001): Application of fast multipole Galerkin boundary integral equation method to crack problems in 3D. *Int. J. Numer. Methods Engrg*, vol. 50, pp. 525–547.

Yoshida, K.; Nishimura, N.; Kobayashi, S. (2001): Application of new fast multipole boundary integral equation method to crack problems in 3D. *Engrg. Anal. Boundary Elements*, vol. 25, pp. 239–247.

Yuji, N.; Hirotada, N.; Tetsuharu, N. (2000): Numerical equivalent inclusion method: a new computational method for analyzing stress fields in and around inclusions of various shapes. *Mater Sci Engng*, vol. A285, pp. 229–238.